Markers of BRCAness in breast cancer

Supplementary Material

Weston R. Bodily[1], Brian H. Shirts[2], Tom Walsh[3,4], Suleyman Gulsuner[3,4], Mary-Claire King[3,4], Alyssa Parker[1], Moom Roosan[5], Stephen R. Piccolo[1,*]

1 - Department of Biology, Brigham Young University, Provo, UT, USA

2 - Department of Laboratory Medicine, University of Washington, Seattle, Washington, USA

3 - Division of Medical Genetics, Department of Medicine, University of Washington, Seattle, Washington, USA

4 - Department of Genome Sciences, University of Washington, Seattle, Washington, USA

5 - Pharmacy Practice Department, Chapman University School of Pharmacy, Irvine, CA, USA

* - Please address correspondence to S.R.P. at stephen_piccolo@byu.edu.

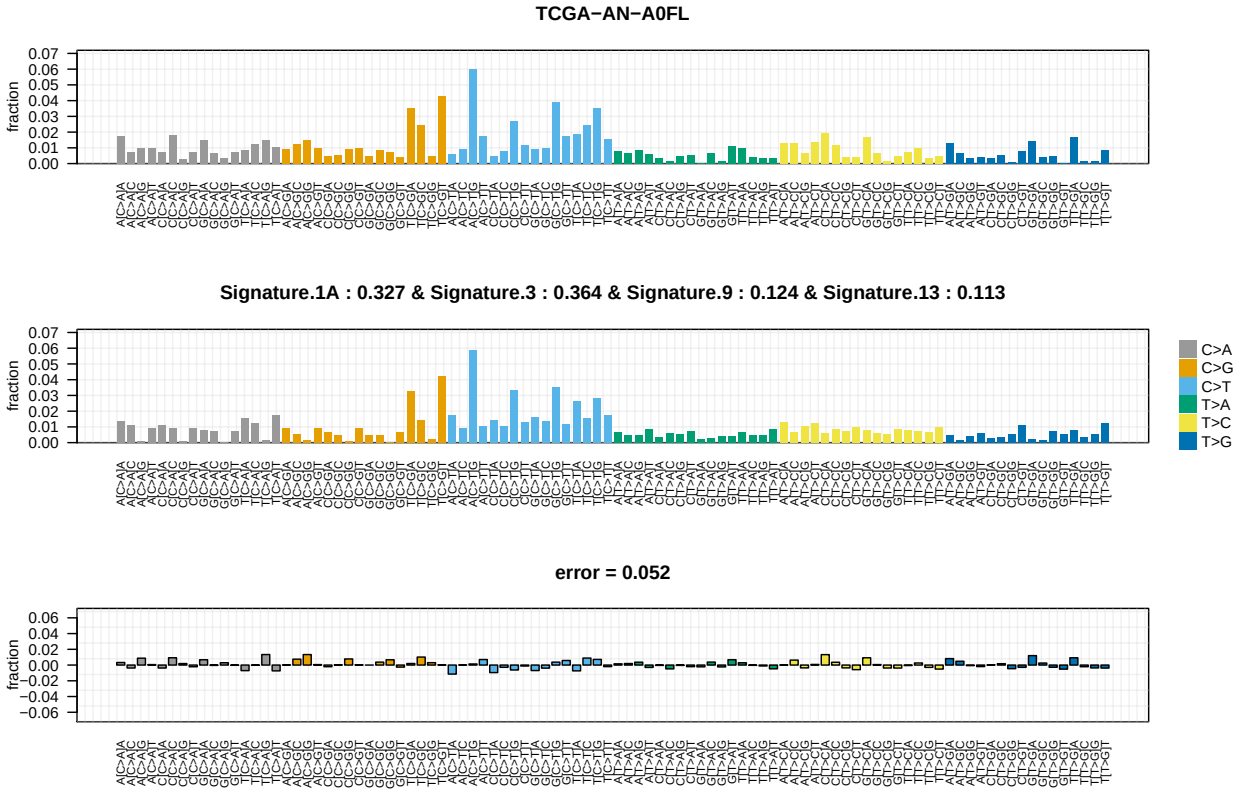

Figure S1: Somatic-mutation signature weights for one Signature 3 tumor. This tumor had a large proportion of C>T mutations, which are representative of Signature 3.

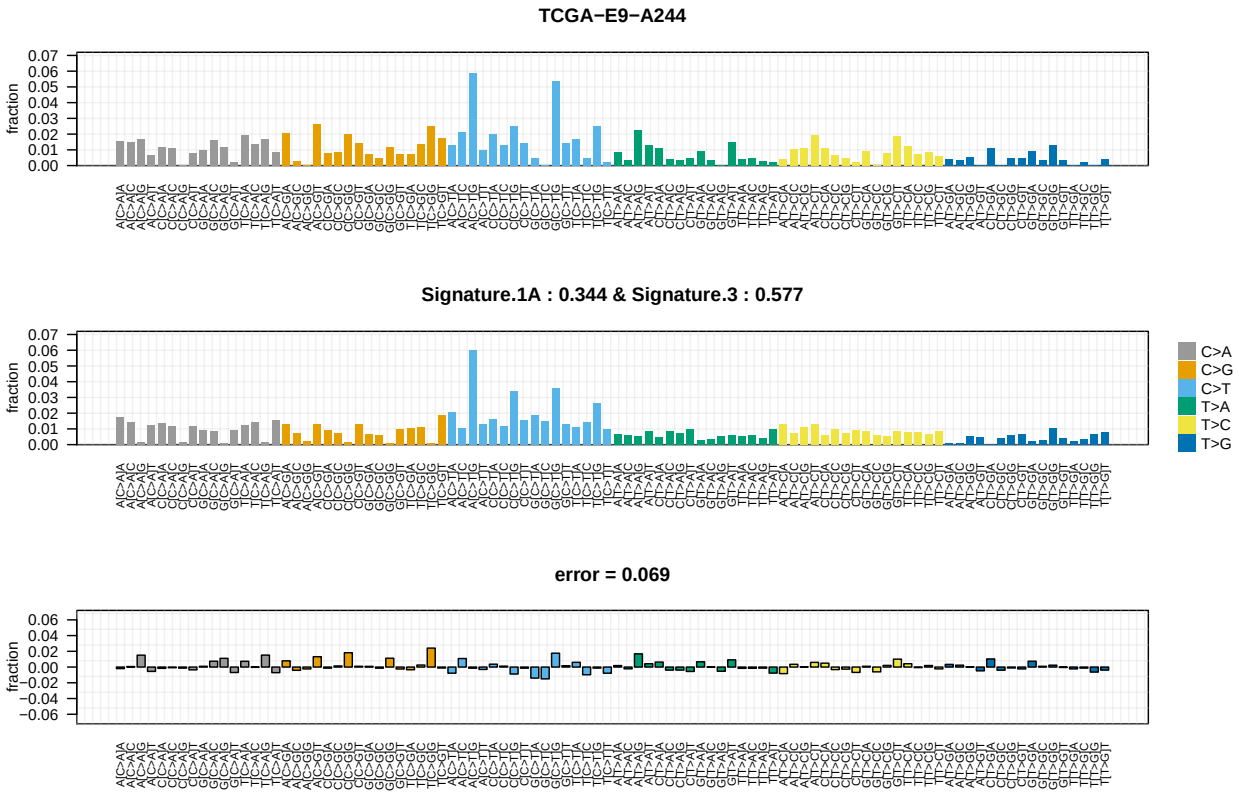

Figure S2: Somatic-mutation signature weights for a second Signature 3 tumor. This tumor had a large proportion of C>T mutations, which are representative of Signature 3.

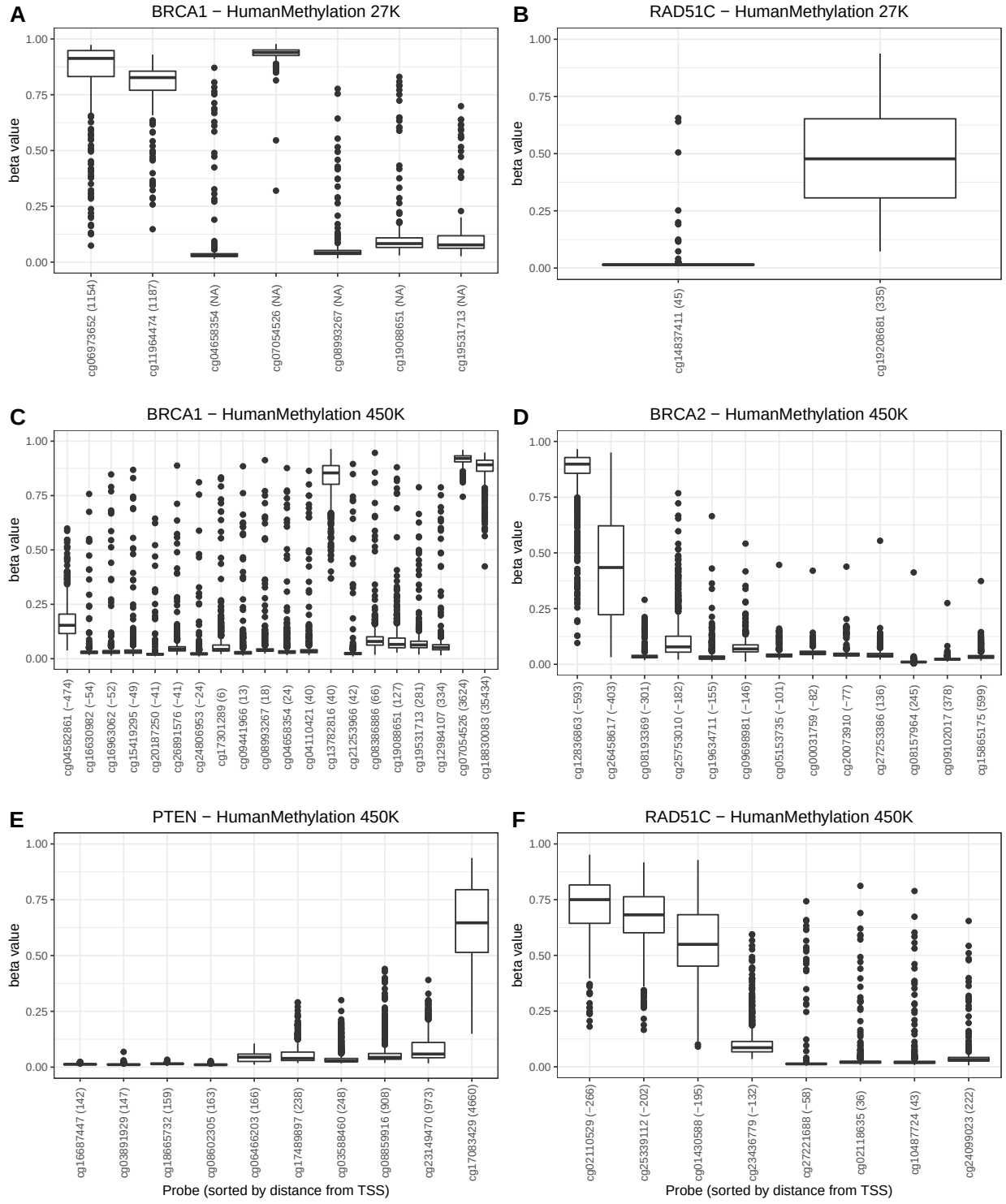

Figure S3: Probe-level summarization of DNA methylation probes. We extracted probe-level methylation (beta) values for all available breast-cancer samples in TCGA and plotted them relative to the transcription start site of each gene. These graphs illustrate beta values for four genes (*BRCA1*, *BRCA2*, *PTEN*, and *RAD51C*) and two microarray platforms (Illumina HumanMethylation 27K and 450K). Values in parenthesis indicate distance from the transcription start site (TSS). TSS distances marked as "NA" were unavailable. The 27K arrays have fewer probes per gene. In

general, probes near the TSS exhibited relatively low methylation levels for these genes, whereas probes further from the TSS were more highly methylated. These observations are consistent with these genes' roles as tumor-suppressor genes, in which we would expect the genes to be "on" by default. Some exceptions to this pattern are apparent (for example, cg13782816 on panel C); these exceptions may be caused by mismapped probes, cross hybridization, or misannotations. We calculated gene-level values as the median across all probes that were within 300 nucleotides of the TSS.

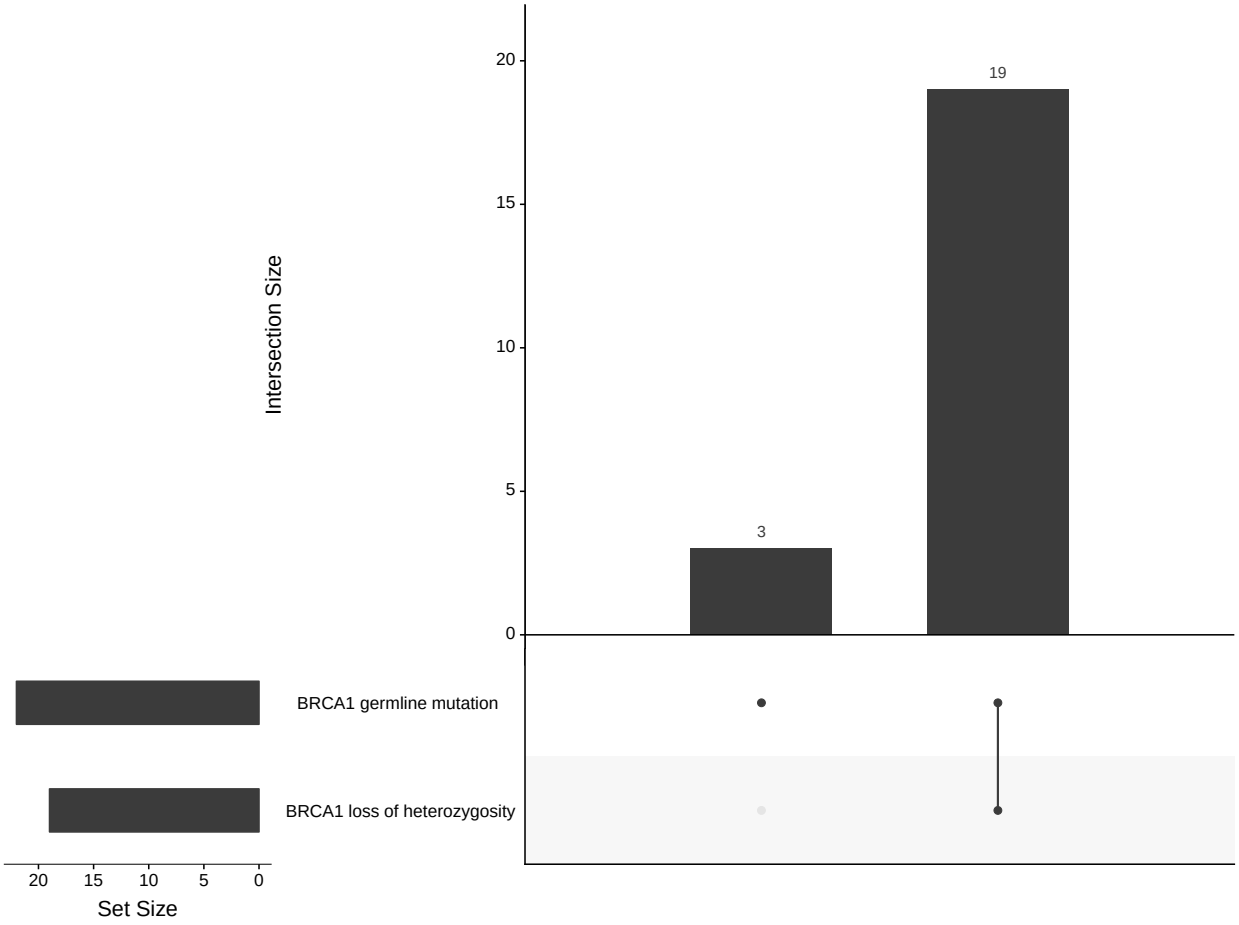

Figure S4: Intersection between germline-mutation status and loss of heterozygosity for *BRCA1*. A total of 22 patients carried a germline mutation in *BRCA1*. We detected loss-of-heterozygosity events in tumors for all but 3 of these patients.

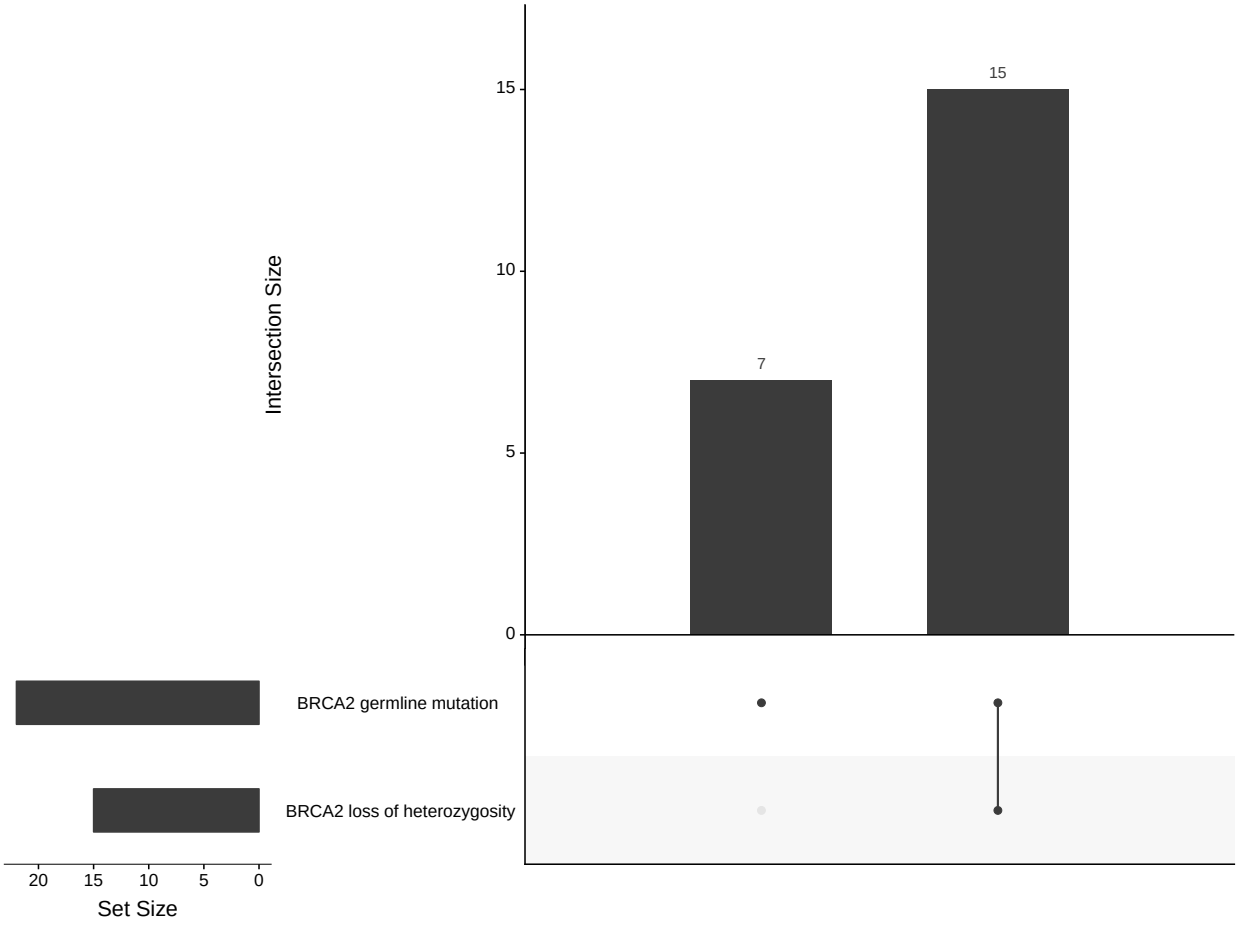

Figure S5: Intersection between germline-mutation status and loss of heterozygosity for *BRCA2*. A total of 22 patients carried a germline mutation in *BRCA2*. We detected loss-of-heterozygosity events in tumors from all but 7 of these patients.

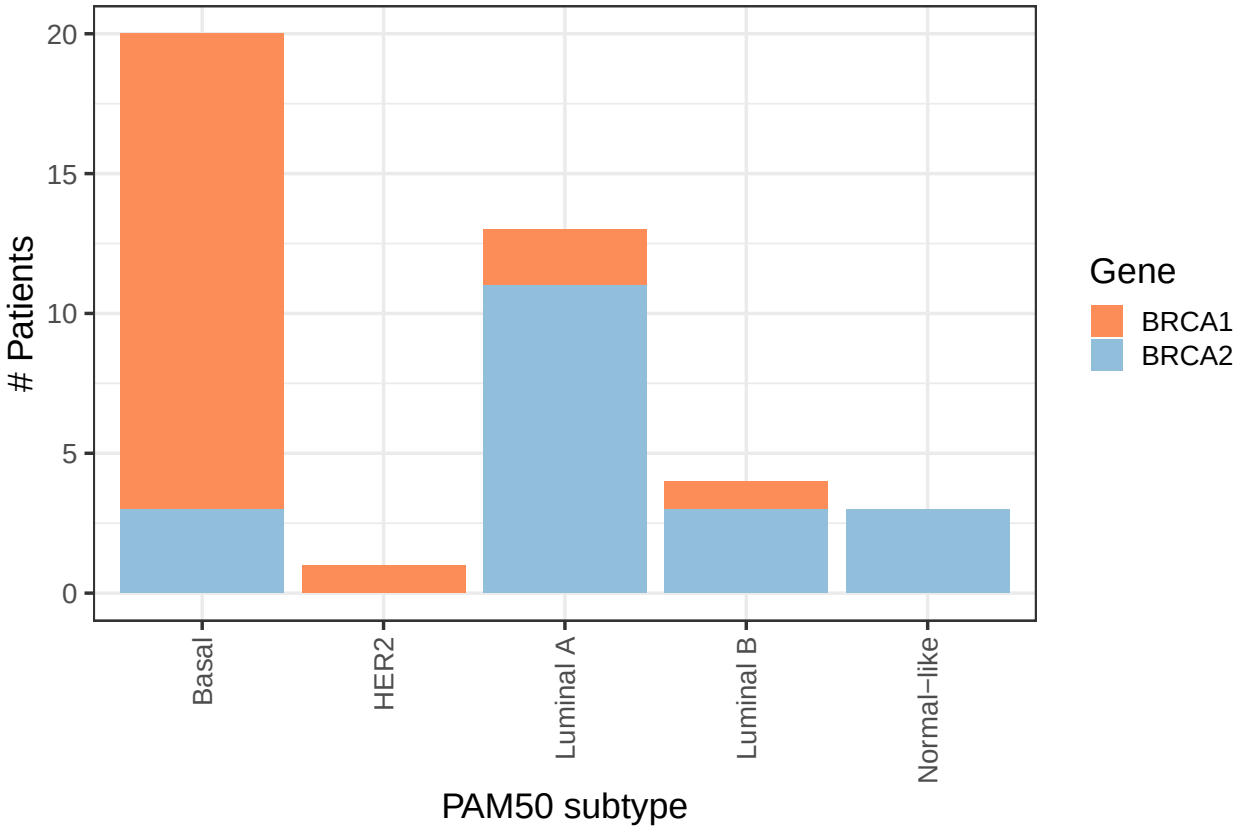

Figure S6: Overlap between *BRCA1*/*BRCA2* germline-mutation status and PAM50 subtype.

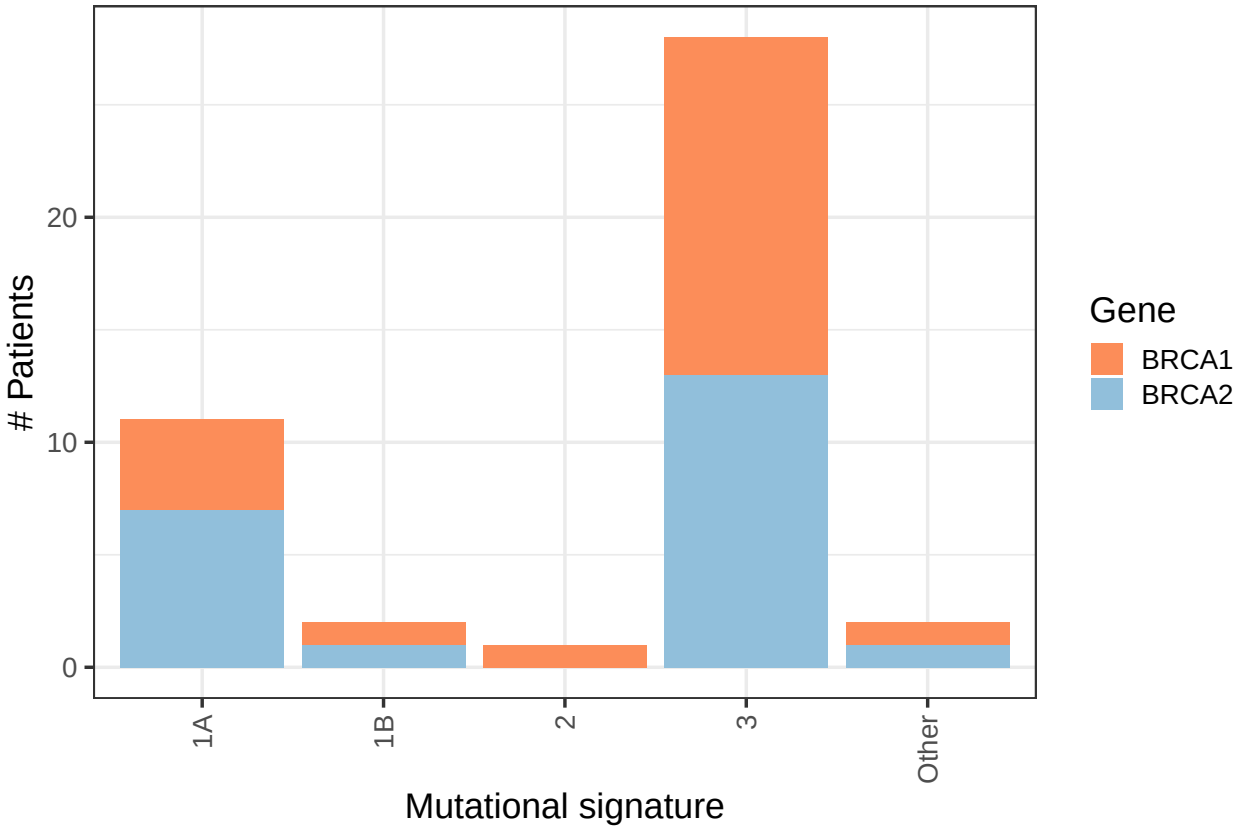

Figure S7: Overlap between *BRCA1*/*BRCA2* germline-mutation status and primary somatic-mutation signature.

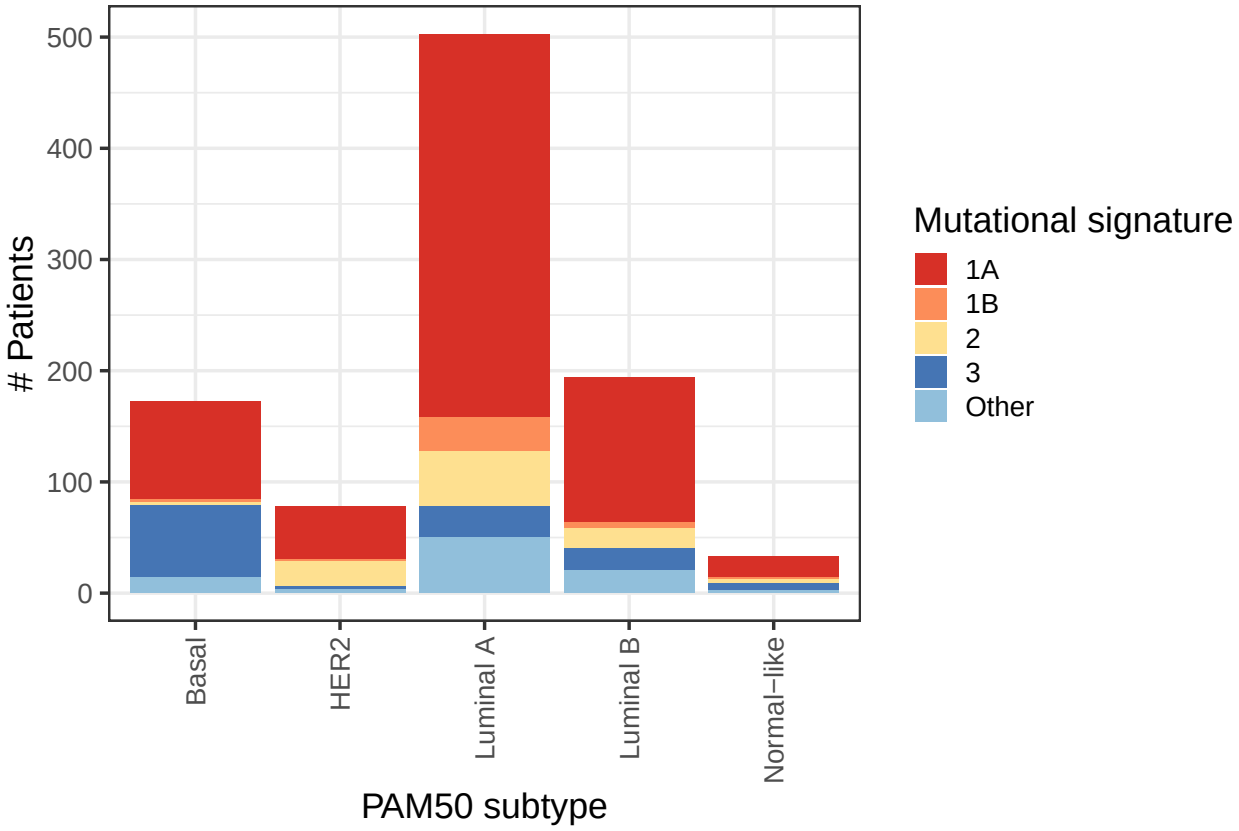

Figure S8: Overlap between PAM50 and primary somatic-mutation signature.

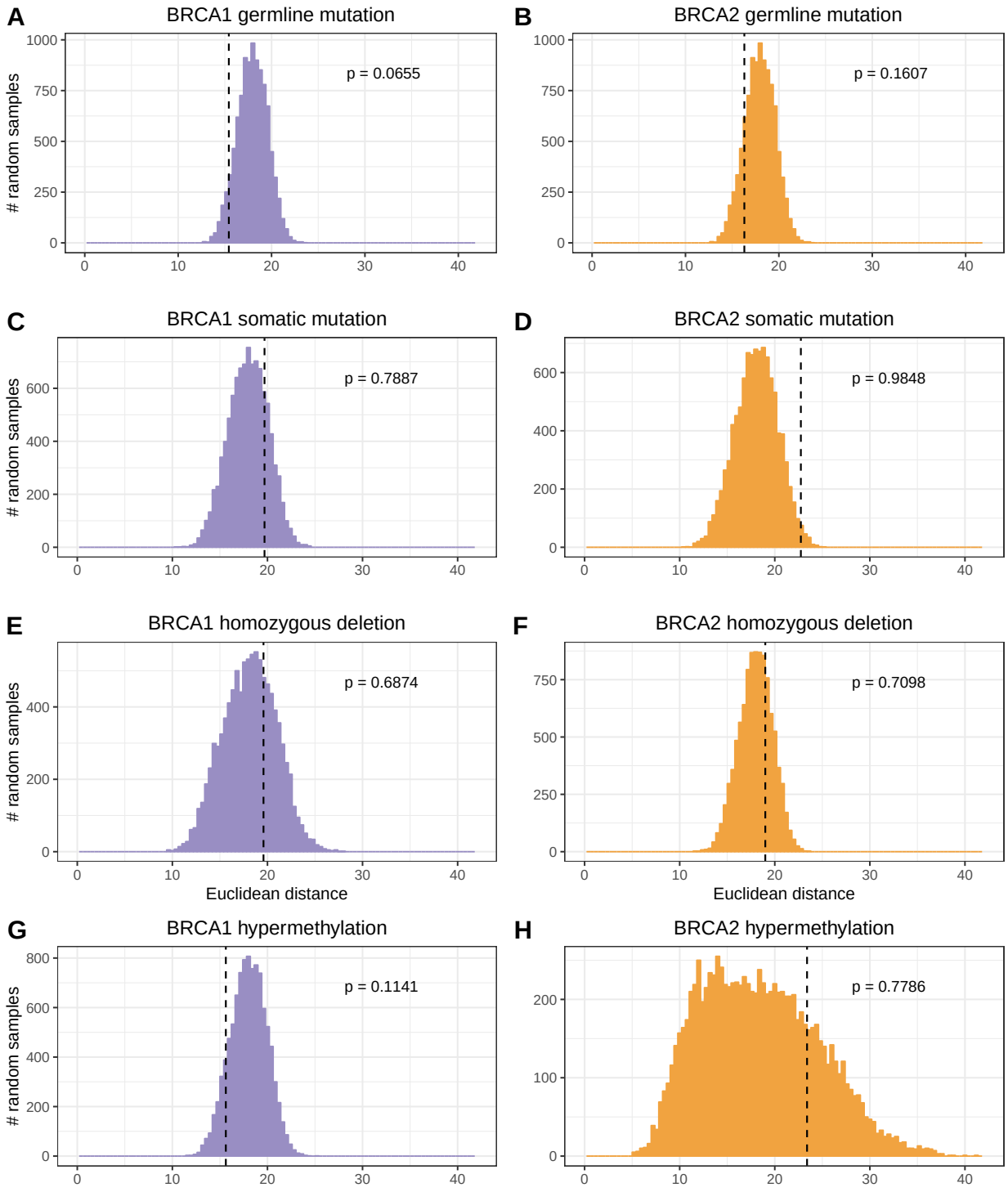

Figure S9: Euclidean distances for randomly selected patients compared to actual distances within *BRCA1*/*BRCA2* patient groups based on PAM50 gene-expression levels. We calculated the Euclidean distance between each pair of individuals who had germline mutations (A, B), somatic mutations (C, D), homozygous deletions (E, F), or hypermethylation events (G, H) in *BRCA1* or *BRCA2*; the medians of these distances are illustrated using vertical, dashed lines. We then randomized the patient identifiers and calculated pairwise distances for the same number

of randomly selected patients, which resulted in an empirical null distribution. We calculated p-values by comparing the actual distances against the randomized distances.

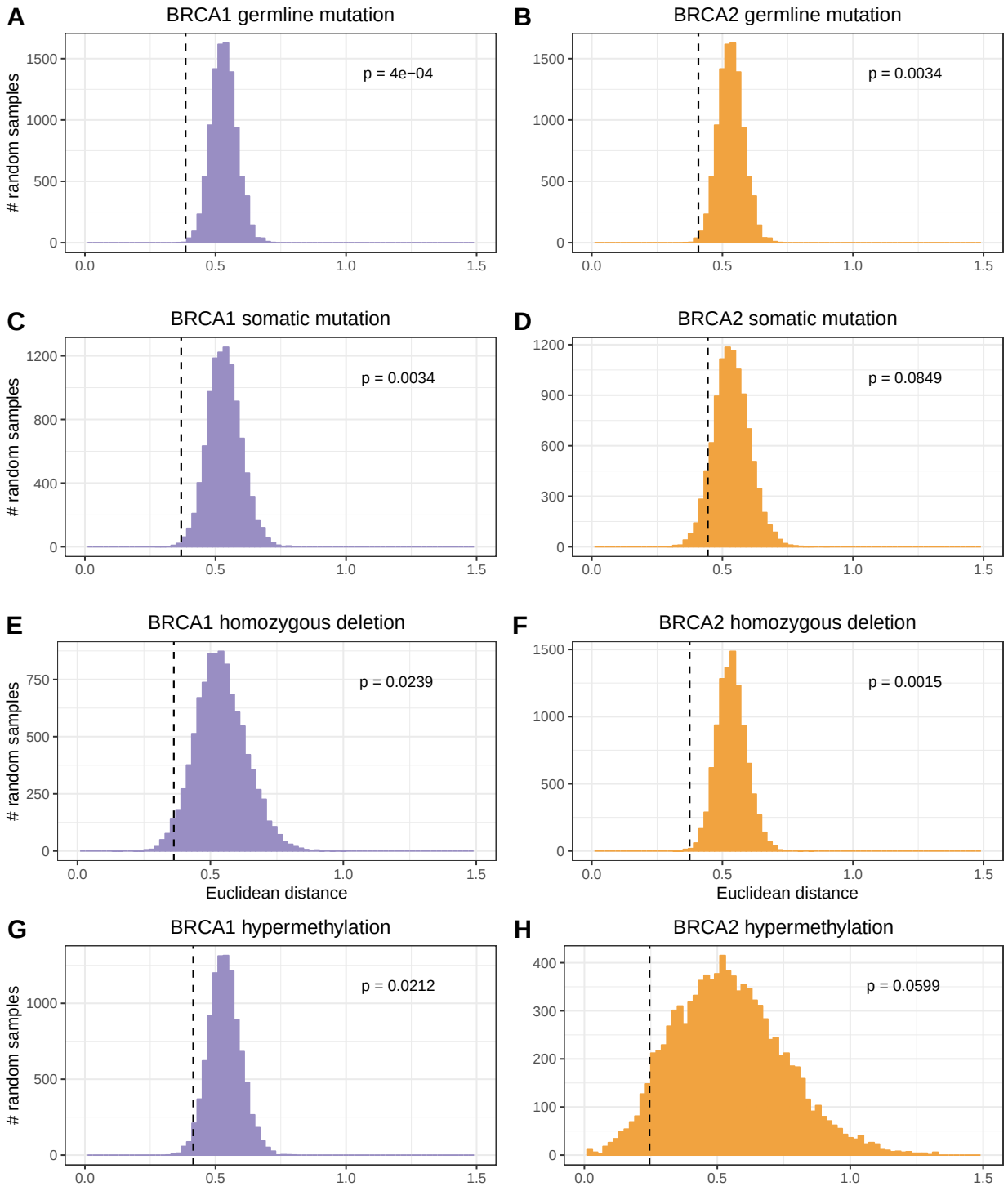

Figure S10: Euclidean distances for randomly selected patients compared to actual distances within *BRCA1/BRCA2* patient groups based on somatic-mutation signatures. We calculated the Euclidean distance between each pair of individuals who had germline mutations (A, B), somatic mutations (C, D), homozygous deletions (E, F), or hypermethylation events (G, H) in *BRCA1* or *BRCA2*; the medians of these distances are illustrated using vertical, dashed lines. We then randomized the patient identifiers and calculated pairwise distances for the same number

of randomly selected patients, which resulted in an empirical null distribution. We calculated p-values by comparing the actual distances against the randomized distances.

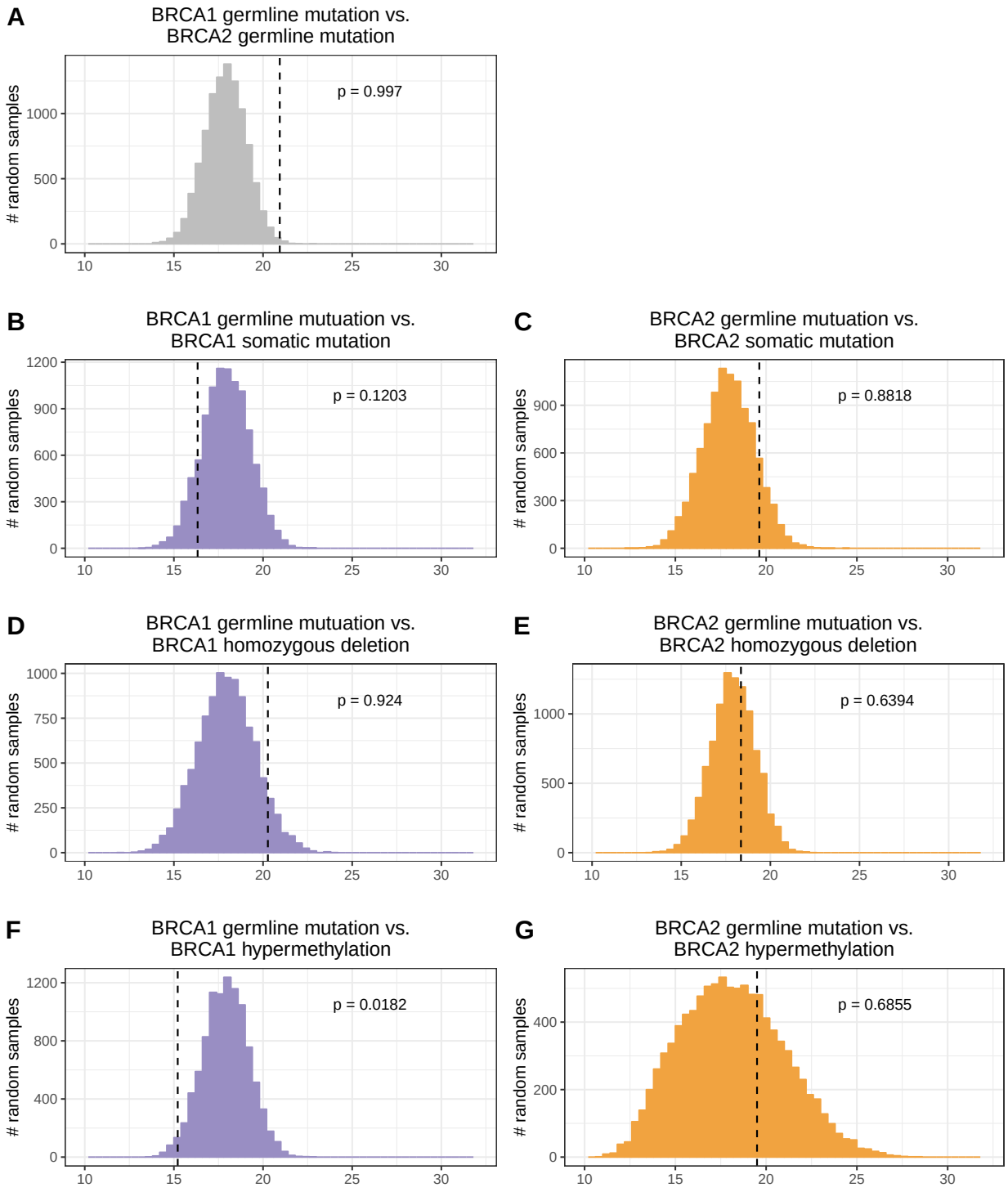

Figure S11: PAM50-based Euclidean distances for randomly selected patient pairs compared to actual distances between patient pairs for individuals with *BRCA1*/*BRCA2* aberrations. We identified patients who had a germline mutation in *BRCA1* or *BRCA2* and compared them against each other (A), those with a somatic mutation in the same gene (B-C), those with a homozygous deletion in the same gene (D-E) and those with DNA hypermethylation of the same gene (F-G). We calculated the Euclidean distance between each pair of individuals in these groups; these

distances are illustrated using vertical, dashed lines. We then randomized the patient identifiers and calculated pairwise distances for groups of randomly selected patients, which resulted in an empirical null distribution. We calculated p-values by comparing the actual distances against the randomized distances.

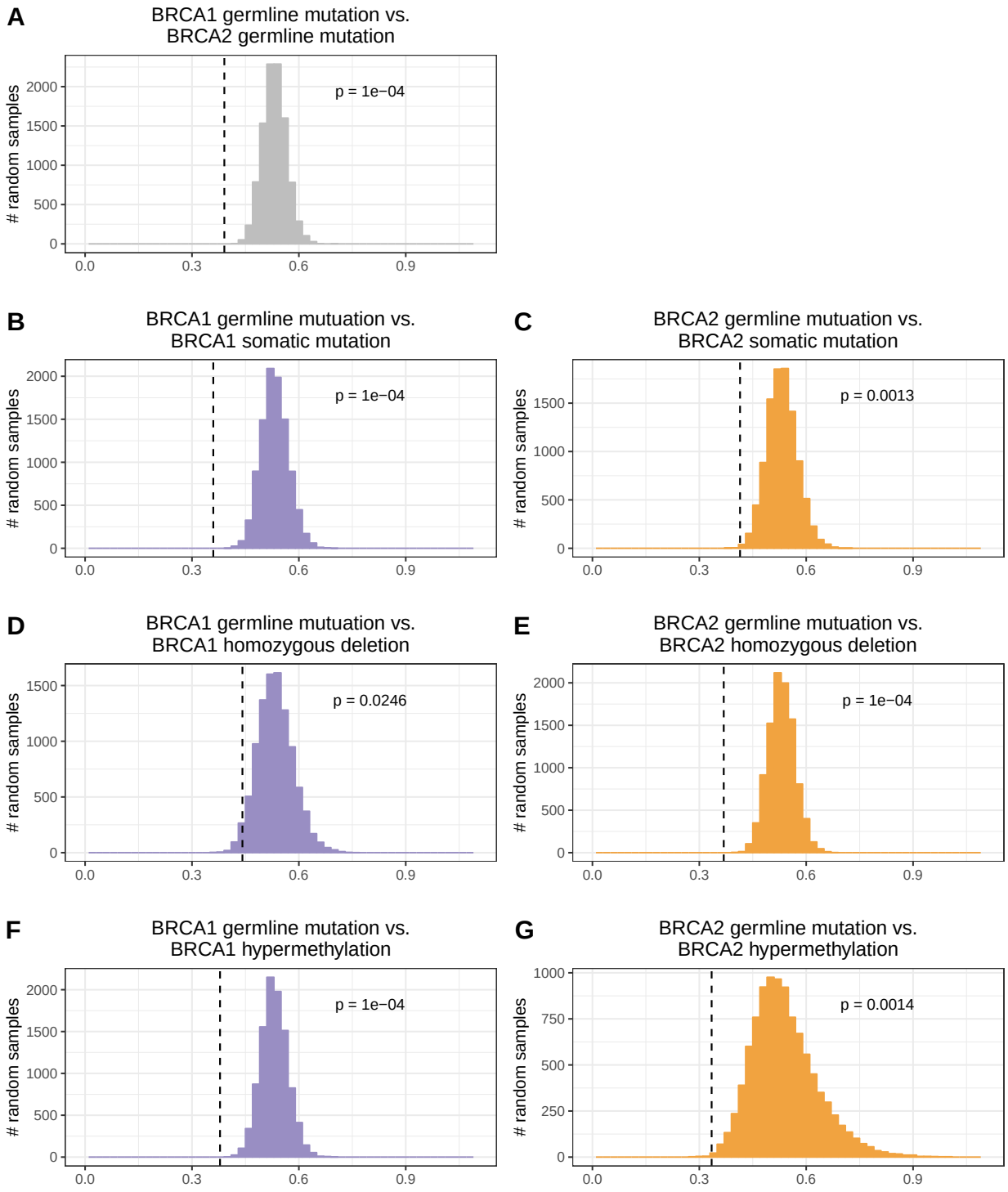

Figure S12: Somatic-mutation signature-based Euclidean distances for randomly selected patient pairs compared to actual distances between patient pairs for individuals with *BRCA1*/*BRCA2* aberrations. We identified patients who had a germline mutation in *BRCA1* or *BRCA2* and compared them against each other (A), those with a somatic mutation in the same gene (B-C), those with a homozygous deletion in the same gene (D-E) and those with DNA hypermethylation of the same gene (F-G). We calculated the Euclidean distance between each pair of

individuals in these groups; these distances are illustrated using vertical, dashed lines. We then randomized the patient identifiers and calculated pairwise distances for groups of randomly selected patients, which resulted in an empirical null distribution. We calculated p-values by comparing the actual distances against the randomized distances.

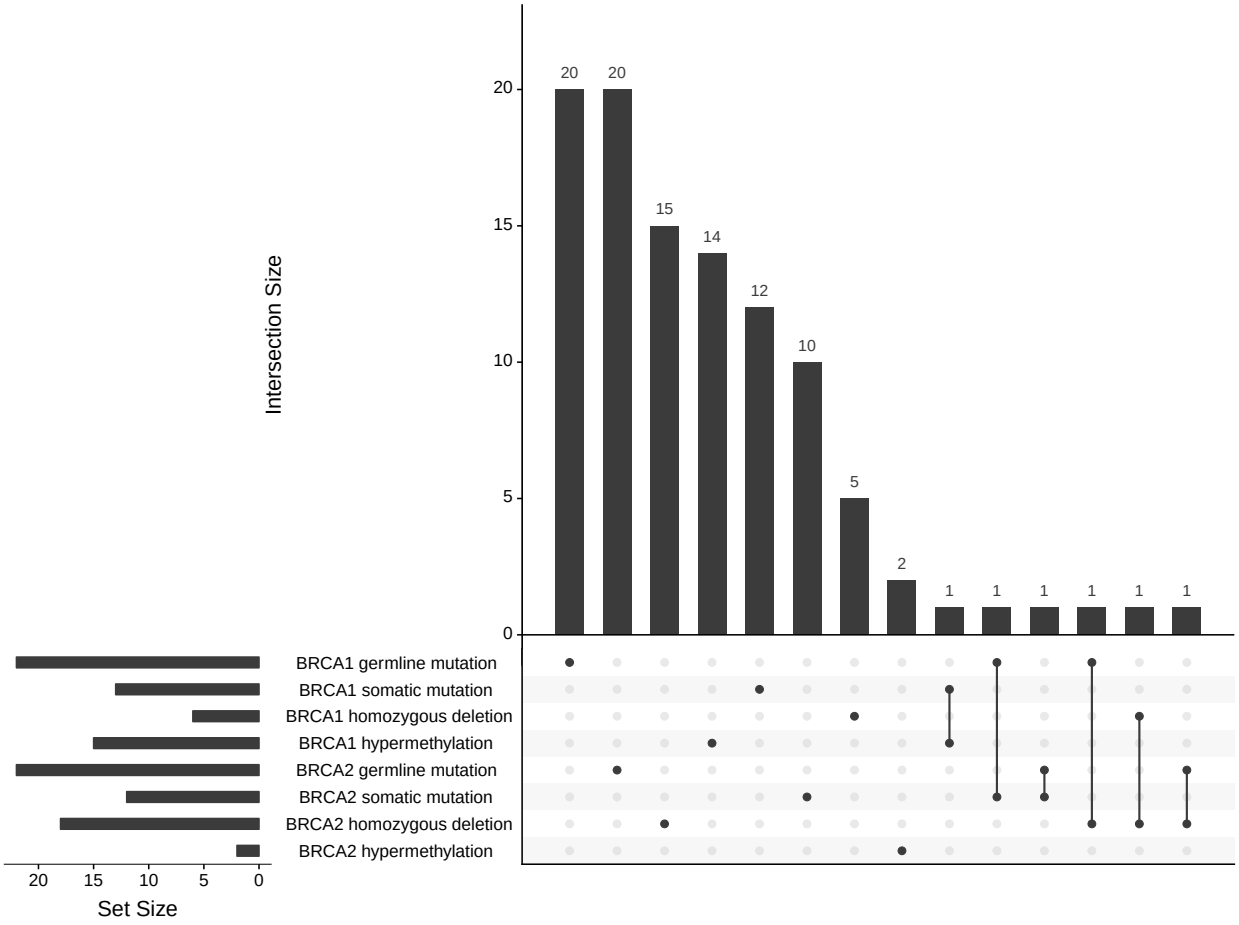

Figure S13: Intersection between different types of molecular aberration in *BRCA1* and *BRCA2*. This graph indicates how many patients had each type of molecular aberration and the level of overlap among these aberrations within a given patient. In most cases, these aberrations were mutually exclusive from each other; however, some overlap did occur. For example, one patient had a somatic mutation in *BRCA1* and hypermethylation of the same gene. This graph only depicts patients for which all four types of molecular data were available.

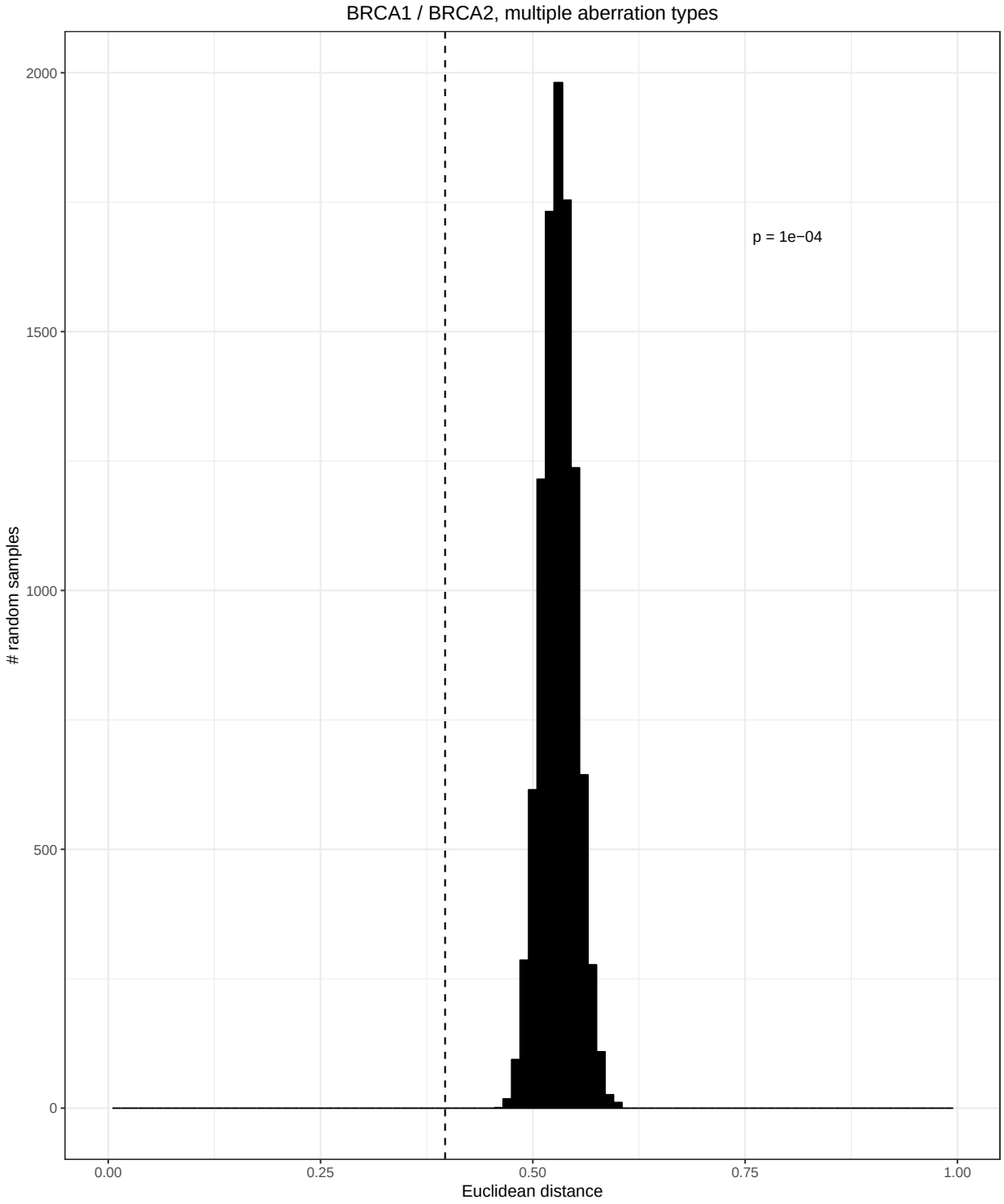

Figure S14: Euclidean distances for randomly selected patients compared to actual distances across all patients with a *BRCA1* or *BRCA2* aberration based on PAM50 gene-expression levels. We calculated the Euclidean distance between each pair of individuals who had a germline mutation, somatic mutation, homozygous deletion, and/or hypermethylation event in *BRCA1* and/or *BRCA2*; the median of these distances is illustrated using a vertical, dashed line. We then randomized the patient identifiers and calculated pairwise distances for the same number

of randomly selected patients, which resulted in an empirical null distribution. We calculated a p-value by comparing the actual distance against the randomized distances.

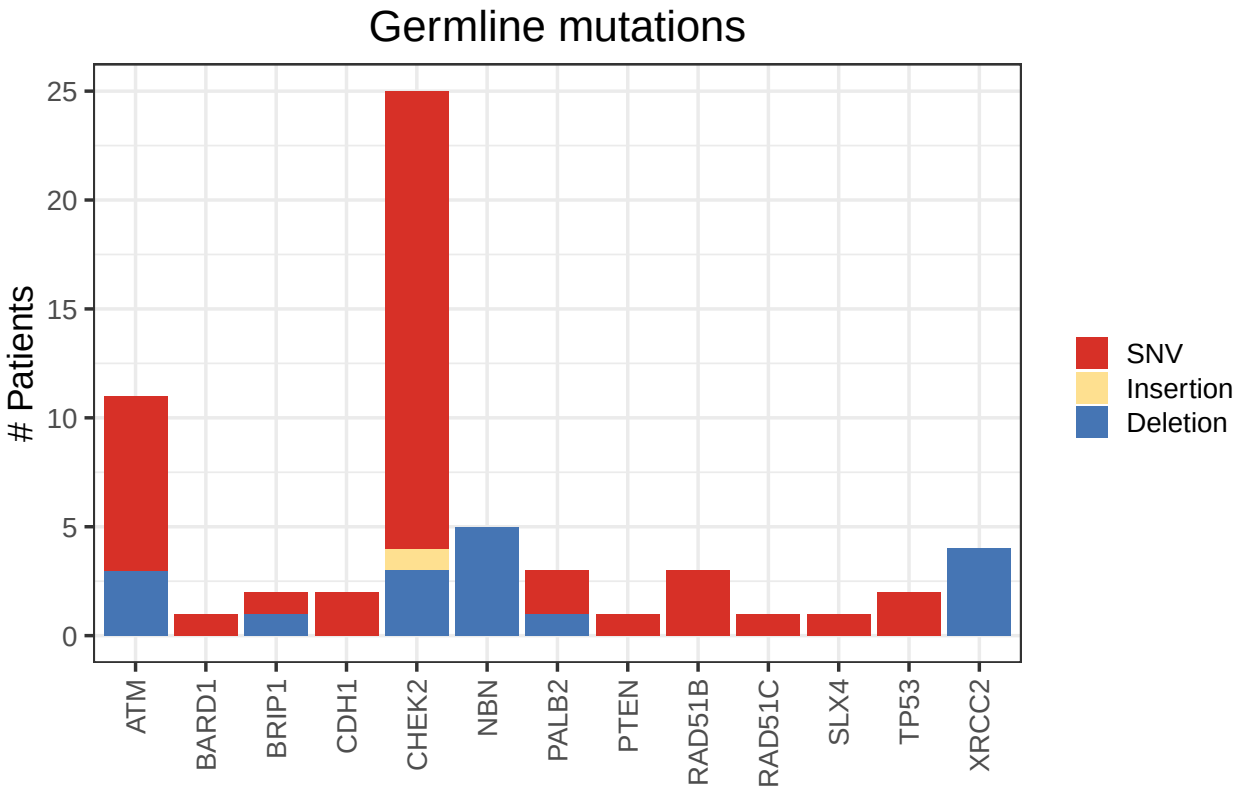

Figure S15: Number of patients with germline mutations in non-BRCA cancer-predisposition genes. This graph omits genes in which we observed no germline mutations. SNV = single-nucleotide variant.

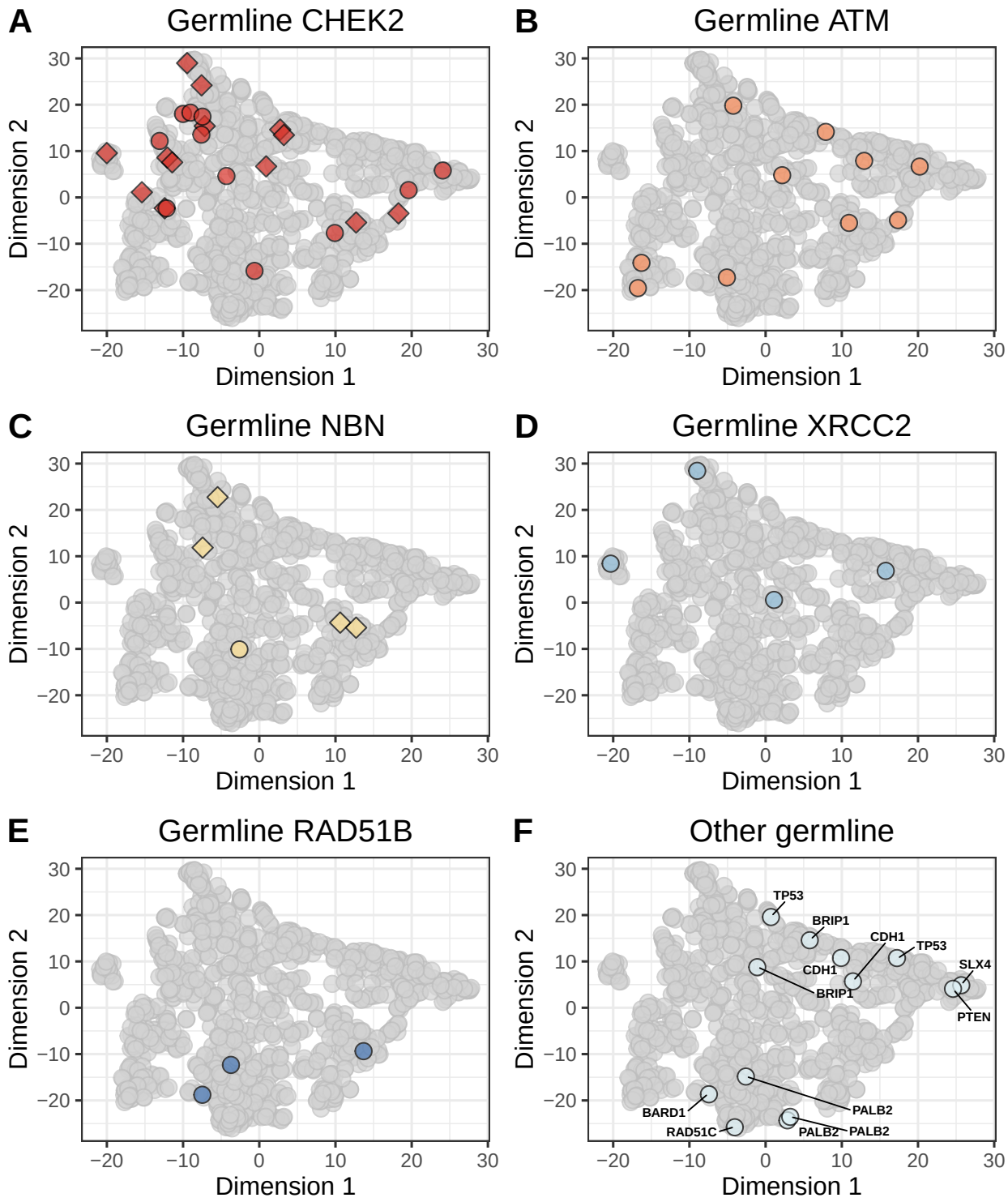

Figure S16: Non-BRCA germline mutations on the somatic-mutation signature landscape. Using the same two-dimensional representation of mutational signatures shown in Figure 3, this plot indicates which patients had germline mutations in non-BRCA cancer-predisposition genes.

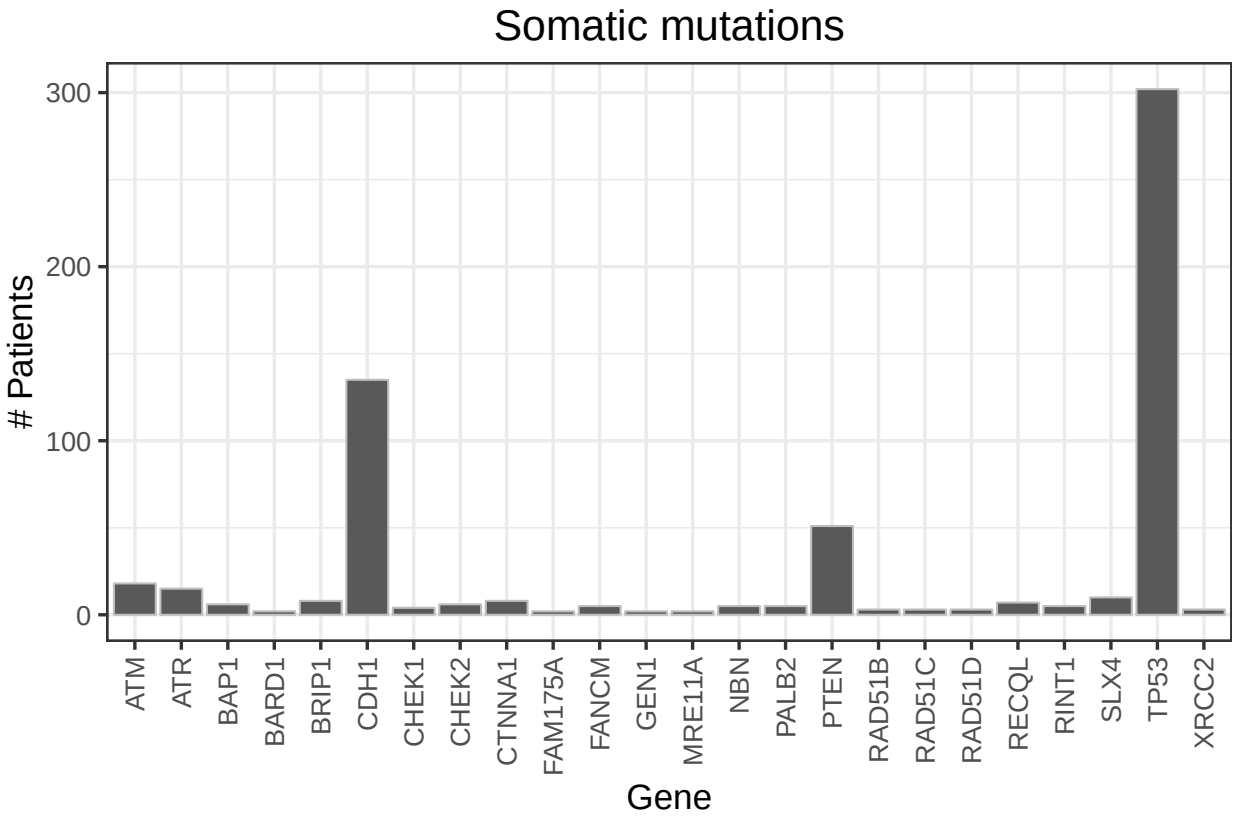

Figure S17: Number of patients with somatic mutations in non-BRCA cancer-predisposition genes. This graph omits genes in which we observed no somatic mutations.

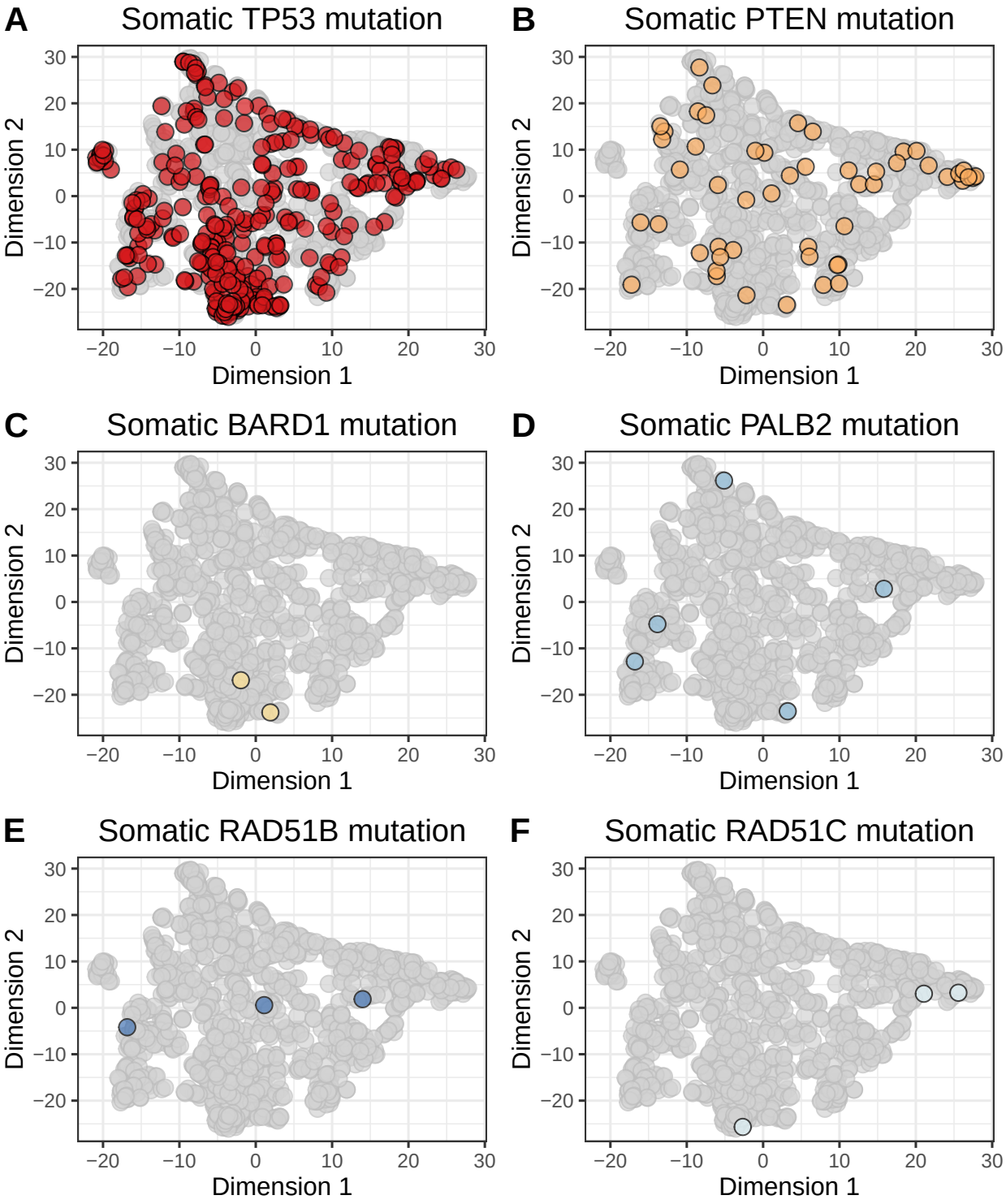

Figure S18: Non-BRCA somatic mutations on the somatic-mutation signature landscape. Using the same two-dimensional representation of mutational signatures shown in Figure 3, this plot indicates which patients had somatic mutations in non-BRCA cancer-predisposition genes.

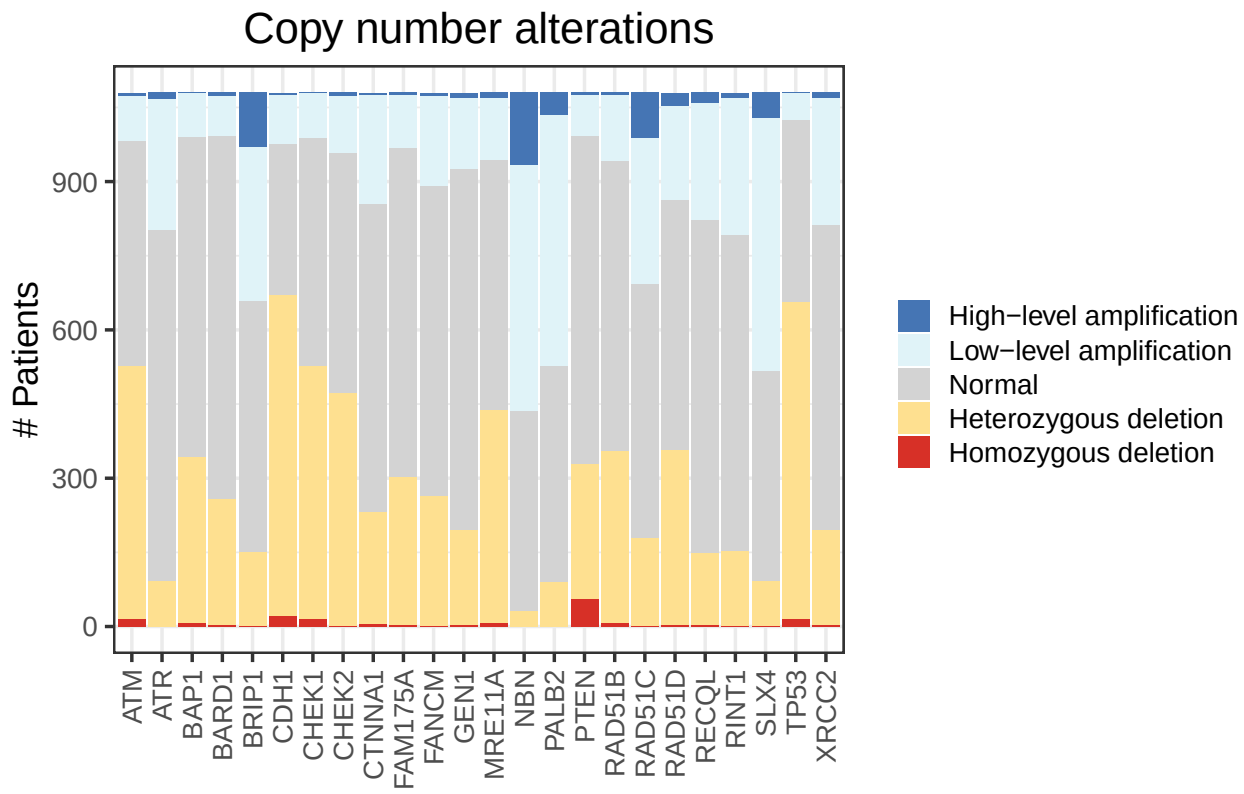

Figure S19: Number of patients with homozygous deletions in non-BRCA cancer-predisposition genes. This graph omits genes in which we observed no homozygous deletions.

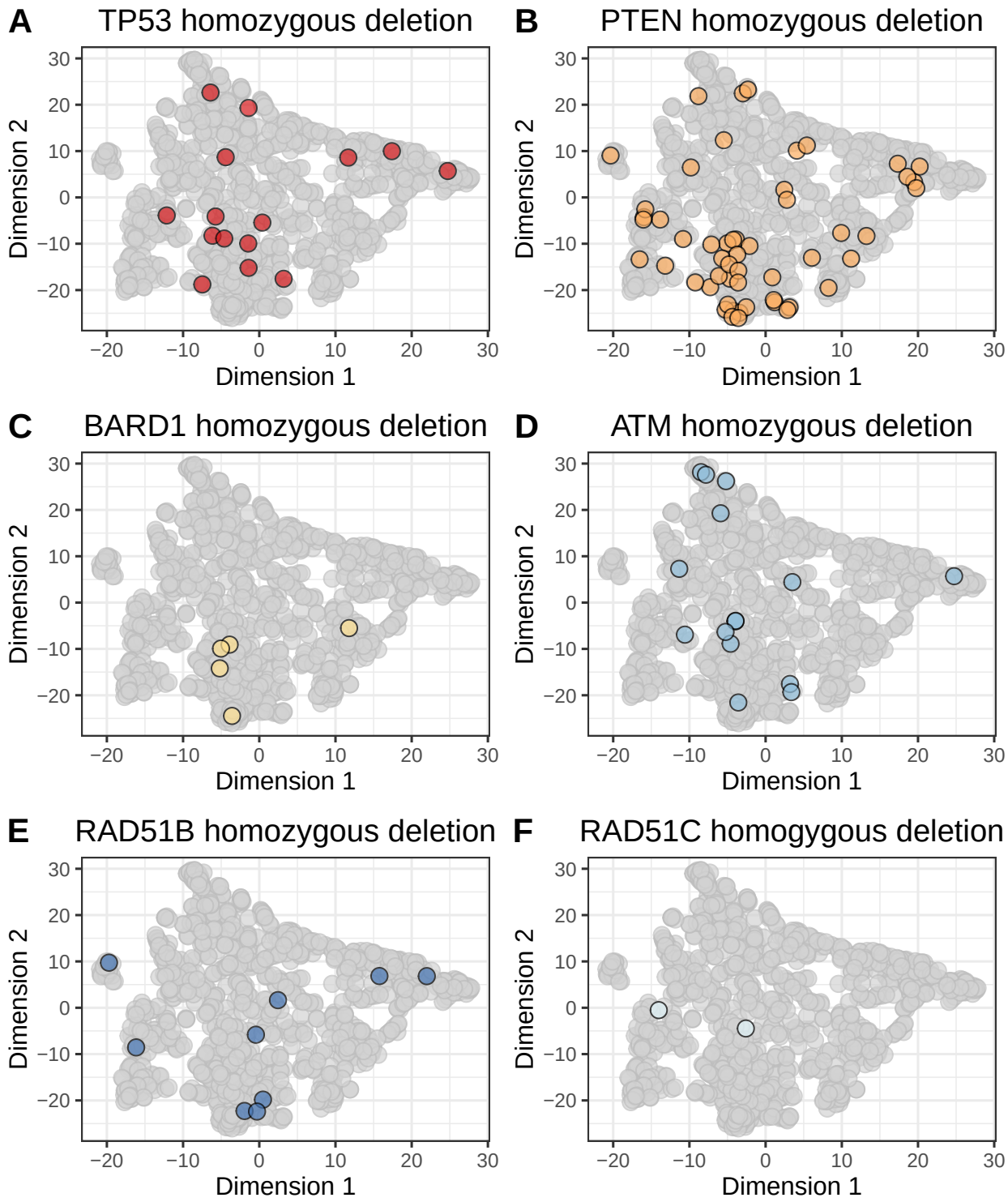

Figure S20: Non-BRCA homozygous deletions on the somatic-mutation signature landscape. Using the same two-dimensional representation of mutational signatures shown in Figure 3, this plot indicates which patients had homozygous deletions in non-BRCA cancer-predisposition genes.

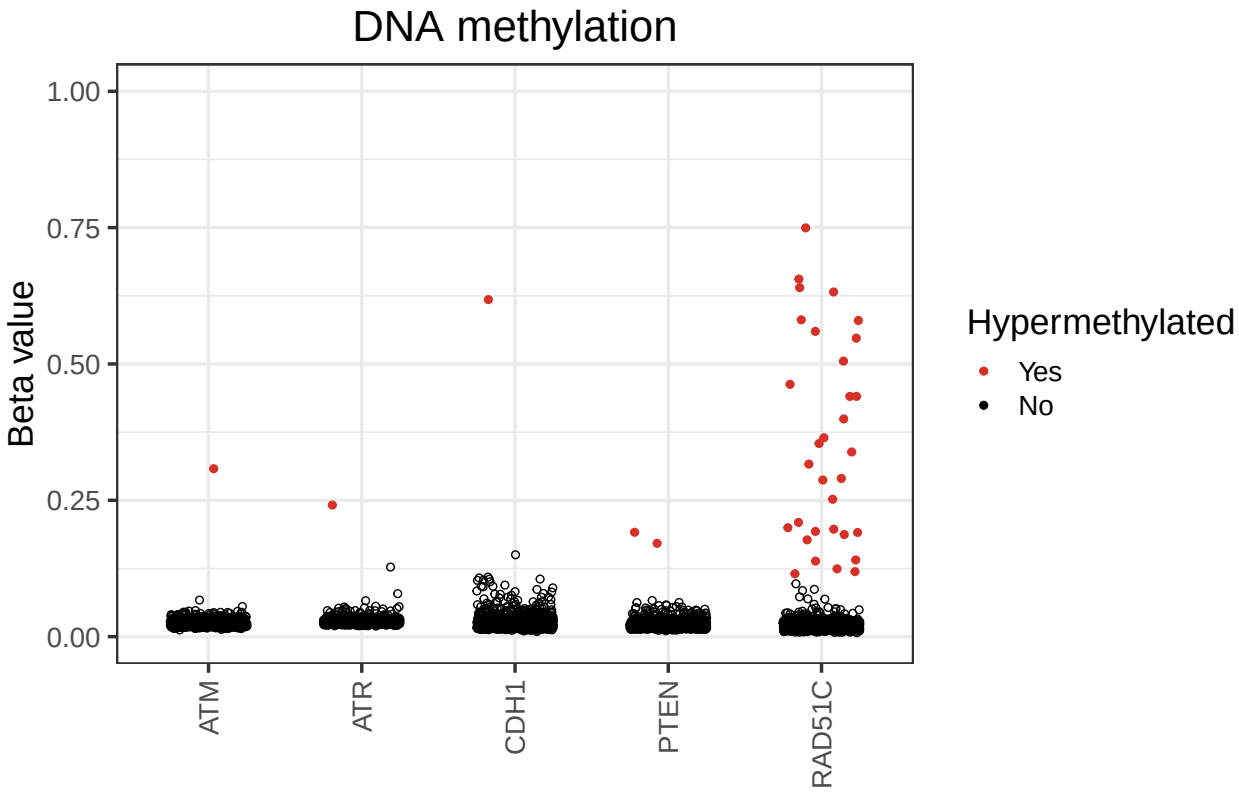

Figure S21: DNA methylation (beta) values for non-BRCA cancer-predisposition genes. Tumors that we classified as having hypermethylation events are highlighted as red points. This graph omits genes in which we observed no hypermethylation events.

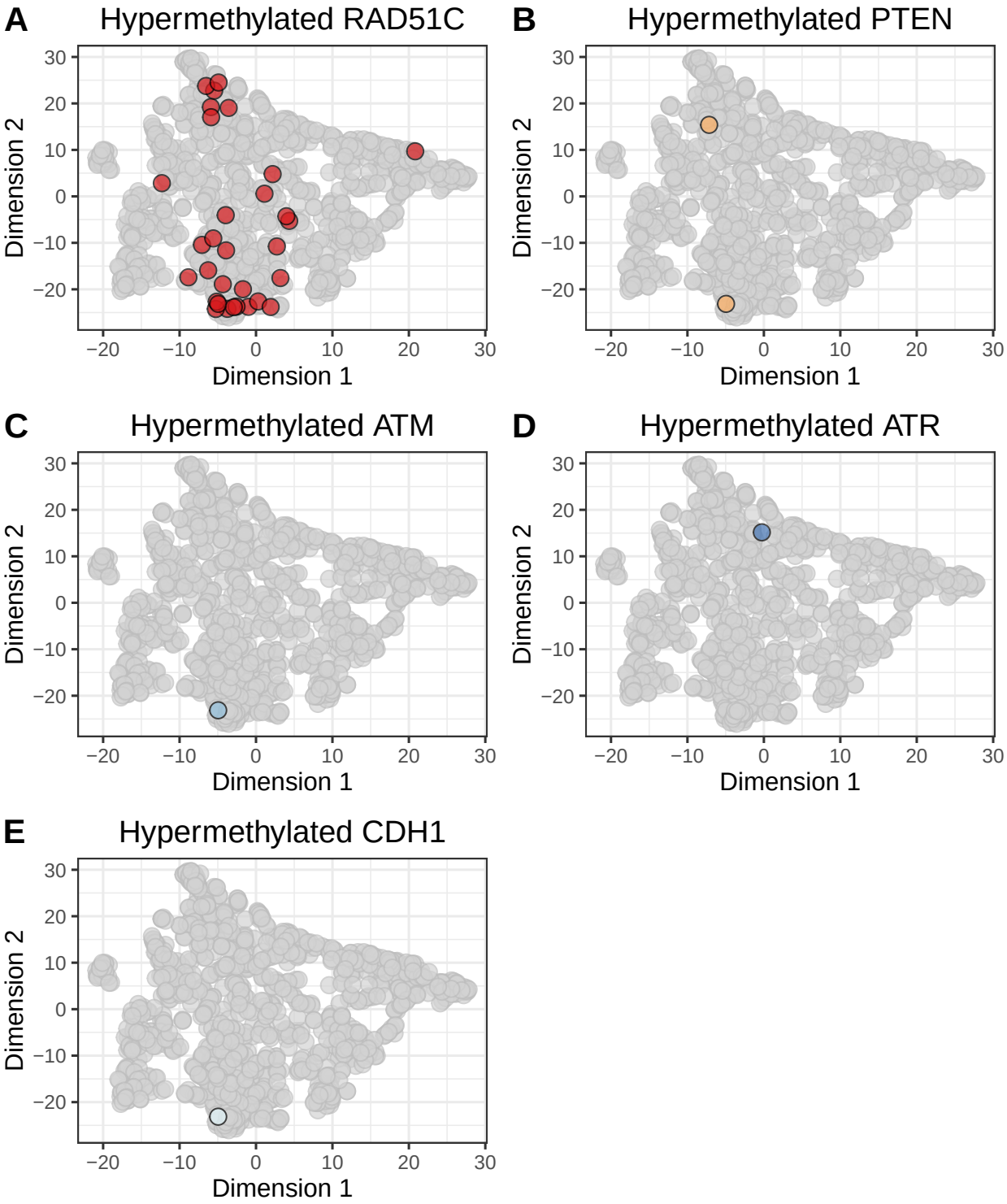

Figure S22: Non-BRCA hypermethylation events on the somatic-mutation signature landscape. Using the same two-dimensional representation of mutational signatures shown in Figure 3, this plot indicates which patients had hypermethylation events in non-BRCA cancer-predisposition genes.

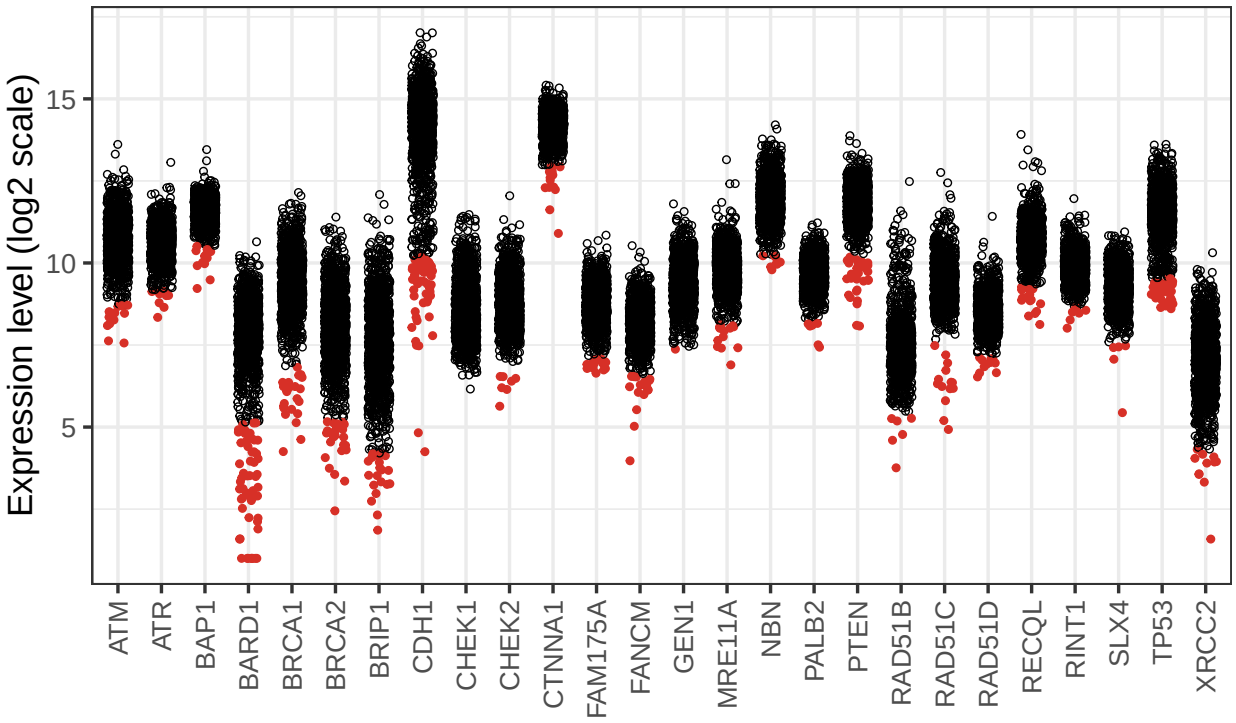

Figure S23: Gene-expression levels for 26 cancer-predisposition genes, including *BRCA1* and *BRCA2*. For each gene, we identified tumors that expressed these genes at relatively low levels compared to other breast tumors; these low expressors are highlighted as red points.

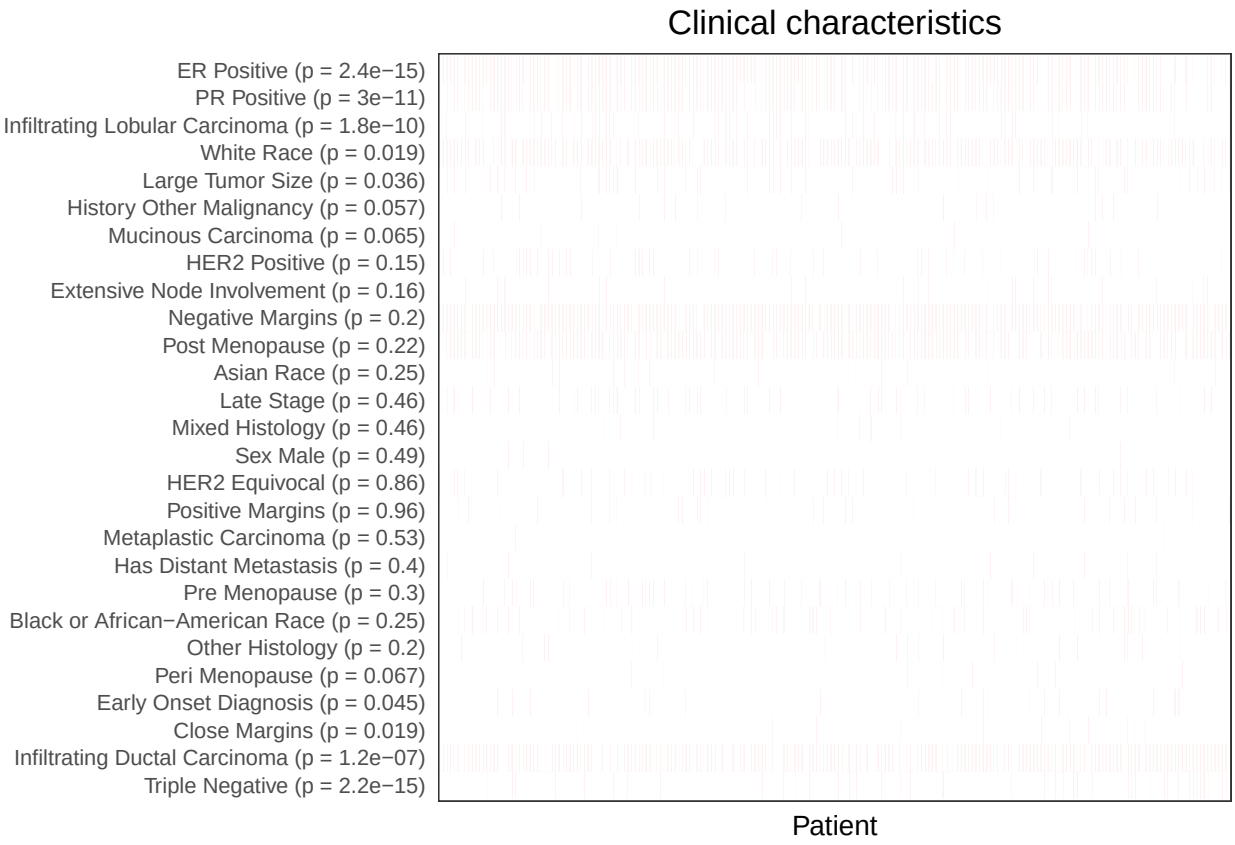

Figure S24: Relationship between BRCA aberration status and demographic, histopathological, and surgical observations in breast-cancer patients. Tumors with triple-negative hormone receptors, infiltrating ductal carcinoma histologies, or close surgical margins overlapped most with BRCA-aberrant tumors based on somatic-mutation signatures.

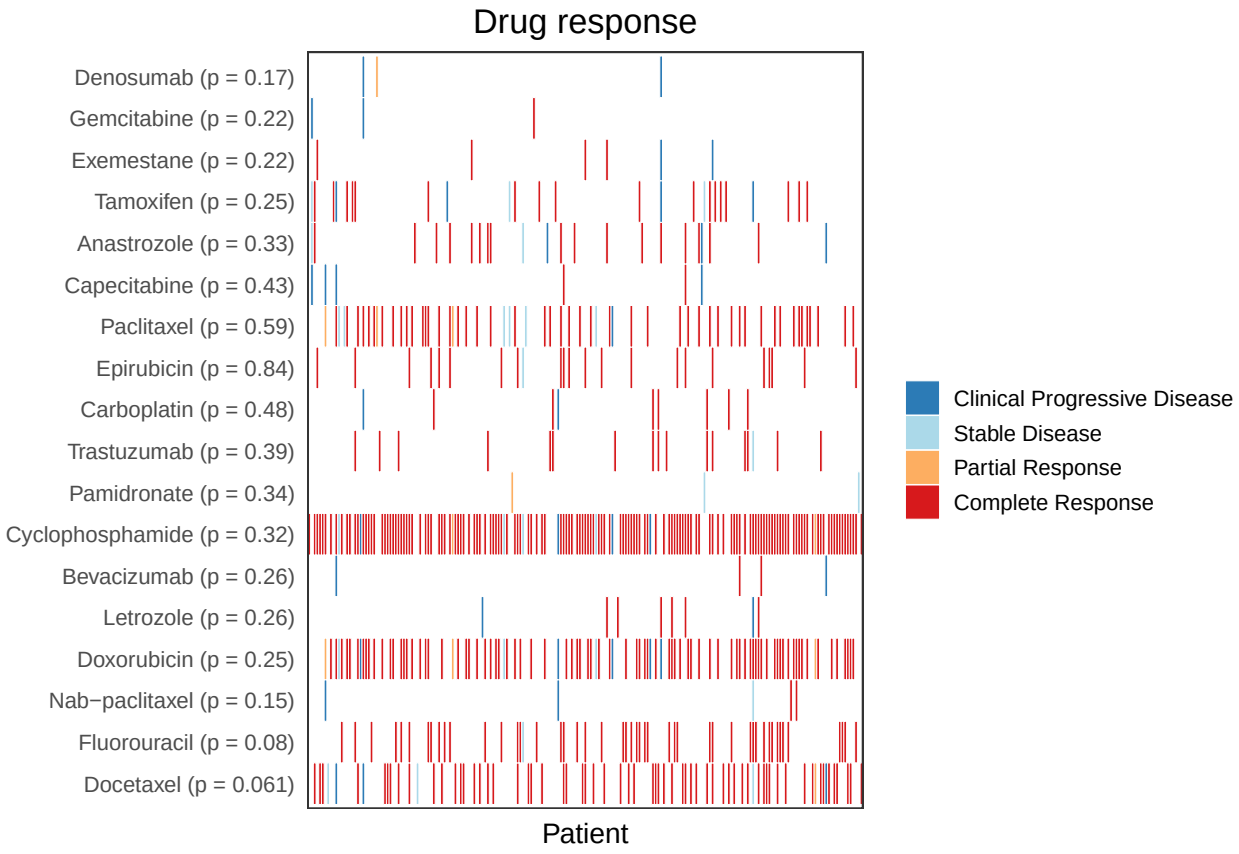

Figure S25: Relationship between BRCA aberration status and pharmacological responses in breast-cancer patients. We evaluated clinical treatment responses for 211 TCGA patients for whom drug-response data were available. Responses for none of the drugs were significantly correlated with BRCA aberration status based on